Clinical Gastroenterologist International

ISSN: 2691-5642

Research Article

Pseudomembranous Colitis with Viral Inclusions and Arenavirus-like Particles

Van Kruiningen HJ[1], West AB[2], Khairallah LH[3], Compton SR[4] and Dreznick JT[5]*

[1]Department of Pathobiology and Veterinary Science, University of Connecticut, USA

[2]Department of Pathology, Yale University Medical School, USA

[3]Department of Physiology and Neurobiology, University of Connecticut, Storrs, USA

[4]Department of Comparative Medicine, Yale University Medical School, New Haven, CT, USA

[5]The Griffin Hospital, USA

Abstract

Background: A 69-year-old man presented for abdominal pain and episodes of diarrhea. He was afebrile, very thin and dehydrated, with distended abdomen. X rays showed dilated large bowel with thickened mucosa. Flexible sigmoidoscopy showed a "continuous circumferential colitis" with some membranous exudate and multiple shallow ulcers. After 26 days he required subtotal colectomy.

Methods: Immunohistochemistry and electron microscopy were employed to define etiology. IHC tested for measles virus, coronavirus, respiratory syncytial virus, rubella, bovine virus diarrhea, influenza and arenaviruses. PCR was done seeking evidence of lymphocytic choriomeningitis virus.

Results: Hematoxylin and eosin and special stains revealed necrosis of colonic crypts. The damage was focal, comprised of dilated crypts containing necrotic cells with granular, globular cytoplasm. These foci were covered with pseudomembranes. Special stains revealed viral intracytoplasmic inclusion bodies. EM demonstrated round and pleomorphic virus particles of 80 nm to 120 nm, with surface spikes and central "ribosomes".

Conclusion: The intracytoplasmic inclusion bodies are similar to those described in arenavirus diseases, and the virus particles seen by EM match those of LCMV in size and shapes, with surface spikes and central "ribosomes".

Keywords: Pseudomembranous colitis; Inflammatory bowel disease; Arenaviruses; Lymphocytic choriomeningitis; Viral inclusions

Introduction

Pseudomembranous colitis is usually caused by *Clostridium difficile* and often as a consequence of treatment with antibiotics [1]. Viral pseudomembranous colitis has been reported infrequently. In 1975 Steer documented a pseudomembranous colitis associated with clindamycin therapy in four patients, two of whom had ultrastructural evidence of virus infection [2]. He noted discrete epithelial ulcers covered by pseudomembranes, and illustrated "atypicality of the colonic epithelium" and ulcers erupting fibrin and polymorphonuclear leukocytes into the colonic lumen. Degenerate surface cells were distended with numerous cytoplasmic vesicles. Round virus particles of 50 nm size and double limiting membrane occurred in damaged epithelial cells and adjacent lumen. These viruses were not identified. Rotavirus, adenovirus and cytomegalovirus have also been identified in pseudomembranous colitis [3,4]. Here we report a patient with severe intractable pseudomembranous colitis that has many similarities to those described by Steer [2].

The patient was a 69-year-old white man, a retired oil worker, who presented for abdominal pain described as crampy, gas-like, non-radiating, and intermittent. He was admitted to Griffin Hospital, Derby CT. Vomiting and diarrhea, approximately four episodes of each, both watery and without blood, occurred two days prior to admission. He had not eaten anything in the past week and was unable to tolerate even water for the previous two days. He was without fever, chills, or muscle aches. He reported no previous episodes like this in the past, and no one else in the home was said to be ill. The patient had been a cigarette smoker, one pack per day, for 40 years and was a binge alcoholic. He was reported to live "rough" periodically. Past medical history indicated previous gastroenterostomy for duodenal ulcer (Billroth II procedure) and surgery for Dupuytren's contracture of the left hand. He had not travelled outside the country for 25 years. However, prior to that he had extensive residence in China, Pakistan, India, and other far-eastern countries. He denied antibiotic use.

Physical examination revealed a normal temperature and stable vital signs. He was very thin, dehydrated, and disheveled, appearing older than his stated age. He had gynecomastia, clubbing of the fingers and toes, Dupuytren's contractures, and testicular atrophy. Other physical signs were within normal limits. His abdomen was mildly distended and without bowel sounds. He was minimally tender to deep palpation, but with no guarding or rebound and no palpable masses. Stool was soft, round, and guaiac negative. The physical examination suggested large bowel obstruction, an infectious process, or colitis. In hospital, significant laboratory data included

Citation: Van Kruiningen HJ, West AB, Khairallah LH, Compton SR, Dreznick JT. Pseudomembranous Colitis with Viral Inclusions and Arenavirus-like Particles. Clin Gastroenterol Int. 2020; 2(1): 1009.

Publisher Name: Medtext Publications LLC

Manuscript compiled: May 09th, 2020

***Corresponding author:** Van Kruiningen HJ, Department of Pathobiology and Veterinary Science, University of Connecticut, Storrs, 61 North Eagleville Road, Unit 3089, CT 06269-3089, USA, Tel: +860-4860837; E-mail: Herbert.Vankruiningen@uconn.edu

fluctuation in electrolyte values, a leukocytosis up to 19,800 and increased segmented neutrophils (76%). Thereafter, the patient's white blood cell counts fluctuated, with a high of 14,700, 18% segmented neutrophils, and 55% band forms. Among chemistry values, the patient consistently had hypoalbuminemia (2.4 mg%, with a normal range of 3.0 mg% to 5.5 mg%). The lowest albumin level obtained was 1.8 mg% 15 days after admission. Other chemistry values were normal, as were repeated blood cultures. Assays for *C. difficile* toxin were negative on three separate occasions and a test for cytotoxin B was negative on two occasions. Examinations for ova and parasites and fecal leukocytes were consistently negative, as were serum titers for *Entamoeba histolytica.*

An abdominal X-ray revealed a dilated large bowel, with a thickened mucosa thought to suggest colitis. A barium enema showed no evidence of colonic obstruction. An upper GI and small bowel series revealed a normal small bowel, but a markedly edematous colon, as evidenced by prominent haustral markings. A barium enema revealed a failure to dilate in the sigmoid and mucosal irregularity and nodulation elsewhere. The descending colon was thin-walled and dilated to 15 cm. CT scan of the abdomen and pelvis also showed severe pancolitis, with what appeared to be an abrupt reduction in diameter between the descending colon and sigmoid, with pericolonic inflammation. The wall of the ascending colon was thickened to approximately five centimeters and that of the sigmoid colon to three centimetres.

Flexible sigmoidoscopy, just beyond the splenic flexure to the distal transverse colon, revealed "some membranous exudate with multiple shallow ulcerations", a "continuous circumferential colitis without gross pseudomembranes". Multiple biopsies of the colon, taken at that time, revealed necrosis, associated with some fibrin, involving the upper two-thirds of the mucosa, with acute inflammation and "focal crypt destruction". Those changes were said to be most suggestive of ischemic colitis. A gastroenterology consult, based on endoscopy and radiographic findings, suggested the patient might have inflammatory bowel disease. The patient was treated with azulfidine, Imodium, and steroids. Stool output decreased from 1000cc to 2500cc daily to 400cc, and the patient was discharged after 22 days in the hospital.

The patient was re-admitted four days later for "ulcerative colitis" that was not getting better. At this time, an indium 111 radiolabeled white blood cell study was done, which demonstrated inflammatory activity in the ascending, transverse, descending, and sigmoid colon, consistent with the patient's history of inflammatory bowel disease. He required subtotal colectomy and ileostomy, and underwent an incidental splenectomy. Gross-examination of the colectomy specimen showed extensive marked acute inflammation with surface erosions, mucinous exudate, and numerous tan-gray fibrinopurulent plaques that measured up to 2.5 cm. Some of the plaques were easily scraped off, but most were adherent to the mucosal surface. The changes were most severe in the more distal portions. The submucosa had edema with some fibrosis. Histologic features were most consistent with a pseudomembranous colitis of some duration. However, an atypical ischemic colitis, ulcerative colitis or an infectious process could not be excluded.

Subsequently the patient was readmitted on several occasions for pulmonary embolus and deep vein thrombosis, but no further intestinal events.

Materials and Methods

Tissues from the colectomy specimen were fixed in 10% neutral-buffered formalin, later processed through a graded series of alcohols and xylene, embedded in paraffin and cut at 4 microns thickness. Stains included hematoxylin and eosin, Brown and Hopps, Macchiavello, Wolbach Giemsa, Modified Steiner, Lendrum's phloxine-tartrazine and Shorr's Page Green. Immunohistochemistry (IHC) was applied, as previously described[5], for measles virus, coronavirus, Respiratory Syncytial Virus (RSV), rubella virus, Bovine Virus Diarrhea Virus (BVDV), Transmissible Gastroenteritis Virus (TGE) of swine and influenza. In 2005, 14 years after the specimens had been taken at surgery, additional IHC was conducted at CDC for Lymphocytic Choriomeningitis Virus (LCMV) and other Old-World arenaviruses. For Electron Microscopy (EM), tissues were fixed in cold 4% glutaraldehyde in 0.1M sodium cacodylate buffer (pH 7.3) for 2 hours, washed and stored refrigerated in 0.2 M sucrose phosphate buffer at pH 7.4. Later the tissues were refixed in 1% osmium tetroxide, immersed for 1 hour in 2% aqueous uranyl acetate, dehydrated in graded ethyl alcohols, and embedded in Epon 812 (Polysciences, Warrington, Pennsylvania, USA). Thin sections were cut with diamond knives and stained with 0.4% lead citrate. Preparations were examined with a Phillips EM 300 electron microscope.

In 2017, 26 years after fixation and embedding of the specimens, PCR was conducted to seek evidence of LCMV, the only likely arenavirus in this region. Formalin fixed paraffin embedded sections of the patient's diseased colon and from the liver from a mouse that had been experimentally infected with lymphocytic choriomeningitis virus (LCMV-Armstrong) were scraped off glass slides. RNA was extracted using the Recover All Total Nucleic Acid Isolation Kit following the manufacturer's instructions (Thermo Fisher Scientific). RT-PCR was performed using the Qiagen One Step RT-PCR kit, 4 ul of extracted RNA and 4 sets of primers specific for the LCMV S gene designed to amplify 189, 157, 180 and 226 bp products: (S1554F: AACAGCGCCTCCCTGACTC and S1743R: TGTGCACTCATGGACTGCAT; S1586F: AGGTGGAGAGTCAGGGAGGC and S1743R; S2140F:CCCTCAATGTCAATCCATG and S2320R:GCATGGGARAACACAACAATTG; S2140F and S2366R:GAAGGATGGCCATACATAGC).

Reaction conditions were: 40 min at 50°C, 15 min at 94°C; 50 cycles of 30s at 94°C, 30s at 50°C, 70s at 72°C; and 10 min at 72°C. RT-PCR products were visualized on a 1% agarose gel using ethidium bromide.

Results

Histologically, the colitis was characterized by foci of cystic crypt dilatation, affecting as few as 6 to 8 crypts in some foci and 12 to 15 in others, immediately adjacent to uninvolved mucosa. The foci of damaged crypts occurred on mucosal ridges (Figure 1) and in mucosal troughs (Figure 2). In these foci, the crypts were denuded, epithelial cells peeled from basement membranes, streaming off, enlarged and granular, lightly caught in mucus (Figure 3). Wispy cells, like detached and disintegrating tissue culture cells, occurred in a mucus matrix, cells strung together two or three at time (Figure 4). Sloughed cells had foamy, granular globular cytoplasm (Figure 5). There were some aggregates of large eosinophilic foamy cells (Figure 5). Remaining epithelium of affected crypts was attenuated, irregularly broken, and

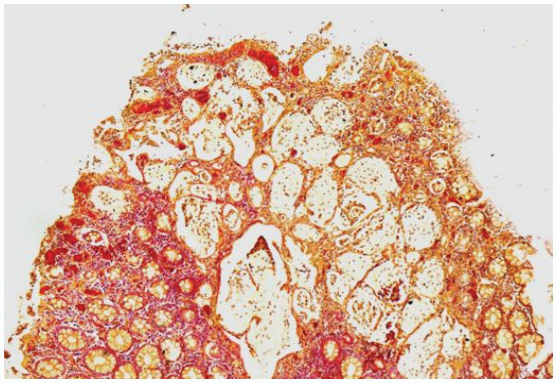

Figure 1: Colonic mucosal ridge. Focally, numerous colonic crypts have attenuated epithelium and contain a variety of necrotic epithelial cells. Adjacent mucosa is congested. Lendrum stain; original magnification 40X.

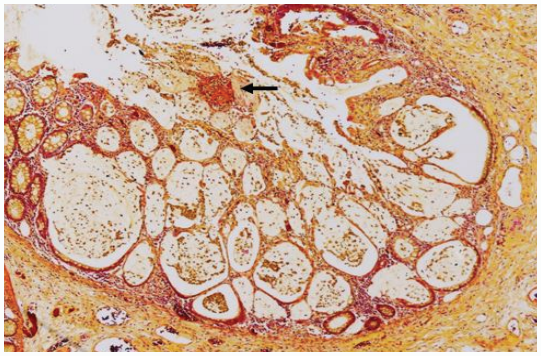

Figure 2: Colonic mucosa in a trough between ridges, with focal crypt cell necrosis and epithelial attenuation. Damaged crypts contain necrotic epithelial cells strung out in mucus. Crypt epithelium at the top is hyperplastic. Arrow indicates a small pseudomembrane. Lendrum stain; original magnification 40X.

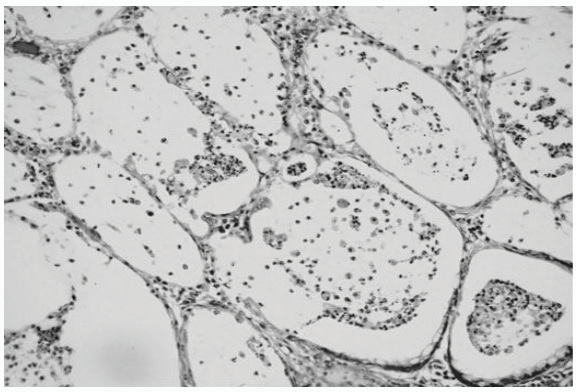

Figure 3: Higher magnification of dilated crypts with attenuated epithelium and various necrotic epithelial cells clumped together in mucus. Shorr's Page Green stain; original magnification 200X.

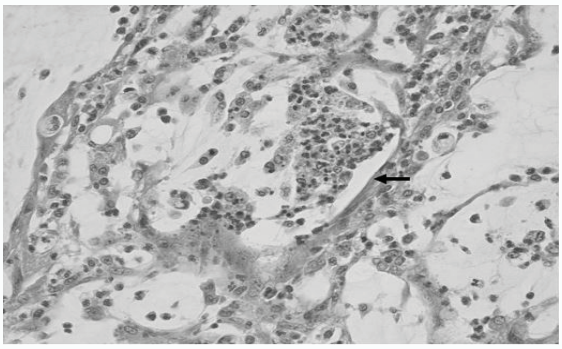

Figure 4: Necrotic crypt epithelial cells, some aggregated, others free within mucus. Arrow indicates attenuated epithelium. Haematoxylin and eosin stain, 400X.

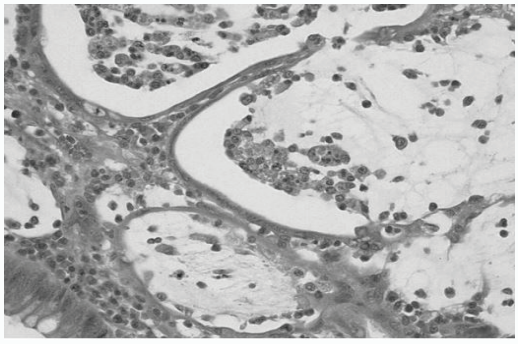

Figure 5: Attenuated crypt epithelium and aggregated granular, globular exfoliated epithelial cells in wispy strands of mucus. H & E, 400X.

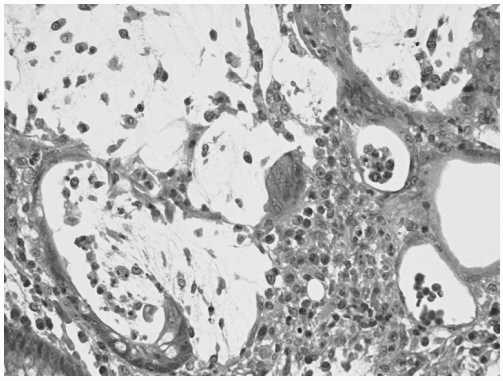

Figure 6: Similar magnification of crypt damage, showing exfoliated and necrotic epithelial cells within wispy strand of mucus. Epithelium at the lower left is hyperplastic; a multinucleated syncytial giant cell occurs at center; lamina propria is rich with plasma cells and small histiocytes. H & E, 400X.

sometimes formed syncytial cells (Figure 6). In other instances, a little hillock of epithelial cells occurred in an otherwise denuded crypt, and there was hyperplasia focally (Figure 6), adjacent to affected crypts. Fibrinous pseudomembranes occurred focally, attached to the reamed and cystic crypts (Figure 2), creating cap-like pseudomembranes at the surface. Page Green and Lendrum special stains revealed rare spherical intracytoplasmic inclusion bodies of one to several micron diameter, occurring singly or as multiples in affected epithelial cells within the damaged crypts. In the Page green preparations, they were orange (Figure 7); in the Lendrum they were hyaline red (Figure 8). Surrounding damaged crypts and in between them there were dilated blood vessels, lymphocytes, plasma cells, and histiocytes (Figure 6). IHC for measles virus, coronavirus, RSV, rubella, BVDV, influenza and arenaviruses were negative.

Electron microscopy revealed virus particles in the cytoplasm of cells of the damaged crypts. The particles ranged in size from 80 nm to 120 nm (Figures 9 and 10); they were round to oval and electron dense, with lighter centers, some of which contained electron

dense internal granules ("ribosomes") (Figure 10). Some were seen budding from intracellular membranes; some were cup-shaped, and others dumbbell-shaped (Figures 10-12). Surface spikes were variably present (Figure 13). Intracytoplasmic Inclusion Bodies (ICIB) were rare (Figure 12).

In the PCR, products of the correct size were obtained with all 4 sets of LCMV primers from the mouse liver sections. Products of the correct size were not obtained from the two samples of human intestinal tissue sections with any of the 4 sets of primers.

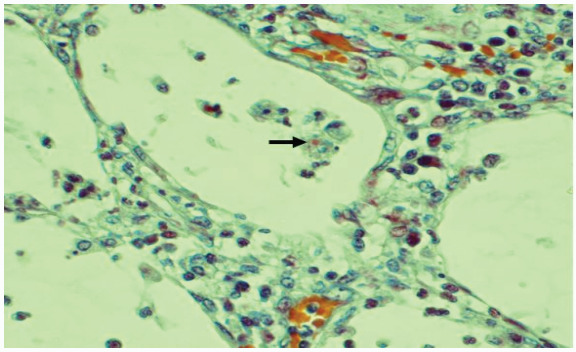

Figure 7: Similar dilated crypts with attenuated epithelium containing enlarged epithelial cells with granular, globular contents and one intracytoplasmic inclusion body (arrow). Shorr's Page Green stain, 600X.

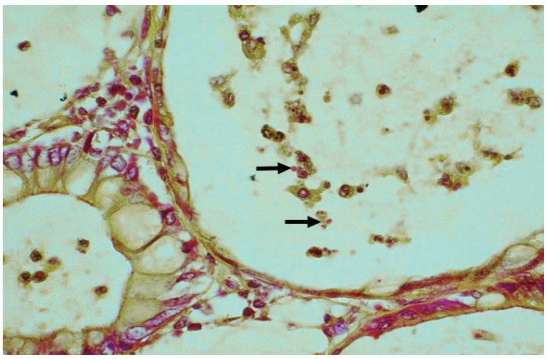

Figure 8: Dilated crypt with attenuated epithelium and multiple intracytoplasmic inclusion bodies (arrows). Lendrum stain, 600X.

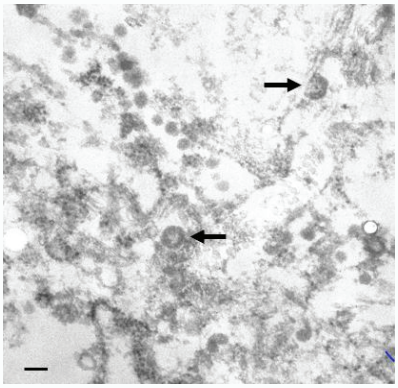

Figure 9: Intracytoplasmic virus particles in a damaged epithelial cell. Particles vary in size. Top arrow indicates a budding particle with central "ribosome"; bottom arrow indicates a cup-shaped virion; kidney bean-shaped particle occurs at bottom center. Bar=100 nm.

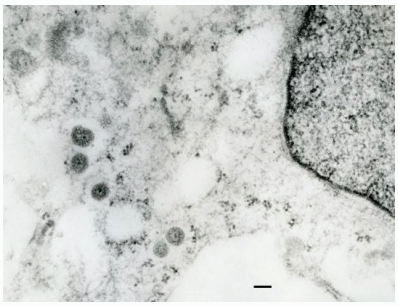

Figure 10: Intracytoplasmic virus particles, each containing a "ribosome". Nucleus is at the right. Bar = 100 nm.

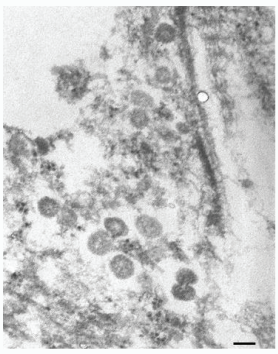

Figure 11: Multiple intracytoplasmic virus particles of 100 nm size, some containing "ribosomes". Dumbbell form at the bottom right occurs in several arenaviruses. Bar = 100 nm.

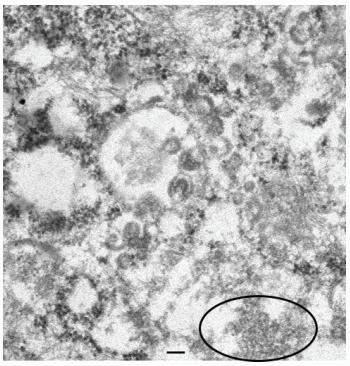

Figure 12: Multiple horseshoe-shaped forms appear to be in the process of forming cup-shaped virions. Oval contains an intracytoplasmic inclusion body. Bar = 100 nm.

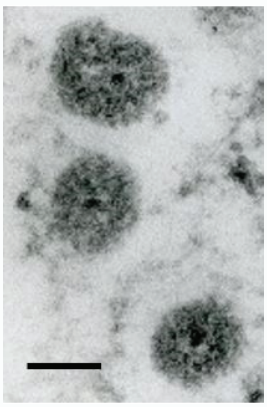

Figure 13: Higher magnification of arenavirus particles with central "ribosomes" and surface spikes. Bar = 100 nm.

Discussion and Conclusion

This unique colitis case was originally studied in 1991, at which time the mucosal changes were seen to resemble virus damage to crypts akin to that of bovine virus diarrhea [6] and bovine coronavirus colitis (winter dysentery) [7,8], hence the initial IHC and EM work-up described above. Electron microscopy at the University of Connecticut revealed some of the virus particles shown here and V. L. Papov at the University of Texas Medical Branch in Galveston demonstrated others. In 2005 we reopened the case; paraffin sections of damaged colon and spleen were submitted to CDC with the expectation that LCMV might be demonstrated. IHC results were disappointing. Colon and spleen were tested employing LCMV antibodies and Lassa virus cross-reactive antibody and evidence of infection was not seen. However, it is now well recognized that prolonged storage of paraffin blocks can result in false negatives [9]. In 2017 PCR failed to demonstrate nucleic acid evidence of LCMV in the aged tissue slices. That finding was, and is, suspect as well, given that RNA degenerates over time in preserved tissues [10].

Thus, we present here histologic and electron microscopic evidence of virus damage to mucosal crypt cells, without IHC or PCR support. Intracytoplasmic inclusion bodies and the viral particles seen on EM are consistent with arenaviruses. The size, shapes (cup forms, kidney bean forms, horseshoe-shaped forms), surface spikes and central "grains of sand" or "ribosomes" are similar to those reported in LCMV by Dalton et al. [11,12] and Muller et al. [13] and similar to those of Machupo virus documented by Murphy et al. [14] The "dumbbell" forms were shown by Dalton [12] and Muller et al. [13] in LCMV and Murphy et al in Lassa virus [15] and Machupo [14]. The ICIBs are identical to those shown in Lassa fever by Walker et al. [16] by light microscopy and to those reported by Dalton [12] (LCMV), Morrison et al. [17] (Lassa), and Murphy et al. [15] (Lassa) by EM. Syncytial cells occur in a number of virus infections [16,18-26], formed by fusion of infected cells with neighboring cells. Multinucleate enlarged cells are induced by surface expression of viral fusion proteins of enveloped viruses [19,23-25]. All of these features suggest that the disease we describe here was the work of an arenavirus. Bell has recently shown Machupo arenavirus antigen uniformly distributed in colonic crypt cells in a guinea pig model [27].

Tang has reminded us that pseudomembranous colitis is not always caused by *C. difficile* [28]. Many of the features in our case resemble those described by Steer [2], in particular the vesicular ballooning of colonic epithelial cells, the localized "atypicality of the colonic epithelium" and the volcanic eruption of focal pseudomembranes. However, the virus particles we demonstrate differ from those shown by Steer. His were round and uniformly 50 nm in size with double limiting membranes, while ours had the many sizes and shapes, surface spikes and central ribosomes of arenaviruses. Because the patient had not been out of the country in 25 years, we believe our evidence implicates an LCMV agent. There are currently more than 30 strains of LCMV, and they vary in pathogenicity [29]. We have presented evidence of a gastroenteric variant.

Acknowledgements

The authors thank Dr. V. L. Popov for electron microscopic consultation; Dr. Salima Haque for initial pathology at Yale; Dr. Stephanie Wain of Griffin Hospital for assistance with retrieval of medical records; Dr. Sharif Zaki and Dr. Jeanette Guarner of CDC for arenavirus immunohistochemistry; Liisa Selin of University of Massachusetts Medical School, Worchester and Dr. Susan Kaech of Yale University for LCMV-positive control mouse tissues; Carl Pedersen of Hartford Hospital and Denise Long of UCONN for IHC; and Jeffrey Magin, Jeremy Doucette and Dr. Joan Smyth for help with the manuscript and images.

Funding

Grant support was from The Broad Medical Research Foundation.

References

1. Simor AE. Diagnosis, management, and prevention of Clostridium difficile infection in long-term care facilities: a review. J Am Geriatr Soc. 2010;58(8):1556-64.
2. Steer HW. The pseudomembranous colitis associated with clindamycin therapy--a viral colitis. Gut. 1975;16(9):695-706.
3. Wenzl TG, Kusenbach G, Skopnik H. Pseudomembranous viral colitis. J Pediatr Gastroenterol Nutr. 2000;30(4):472.
4. Franco J, Massey BT, Komorowski R. Cytomegalovirus infection causing pseudomembranous colitis. Am J Gastroenterol. 1994;89(12):2246-8.
5. Cartun RW. Immunohistochemistry of infectious diseases. J Histotech. 1995;18:195-202.
6. Uzal F, Plattner B, Hostetter J. Alimentary system. Jubb, Kennedy and Palmer's pathology of domestic animals. Volume 2. Sixth ed. 2016:1-88.
7. Van Kruiningen H. Gastrointestinal system. In: RG Thomson, ed. Special Veterinary Pathology. 1998:186-7.
8. Van Kruiningen HJ, Khairallah LH, Sasseville VG, Wyand MS, Post JE. Calfhood coronavirus enterocolitis: a clue to the etiology of winter dysentery. Vet pathol. 1987;24(6):564-7.
9. Economou M, Schoni L, Hammer C, Galvan JA, Mueller DE, Zlobec I. Proper paraffin slide storage is crucial for translational research projects involving immunohistochemistry stains. Clin Transl Med. 2014;3:4.
10. Klopfleisch R, Weiss AT, Gruber AD. Excavation of a buried treasure--DNA, mRNA, miRNA and protein analysis in formalin fixed, paraffin embedded tissues. Histol histopathol. 2011;26(6):797-810.
11. Dalton AJ, Rowe WP, Smith GH, Wilsnack RE, Pugh WE. Morphological and cytochemical studies on lymphocytic choriomeningitis virus. J Virol. 1968;2(12):1465-78.
12. Dalton AJ, Haguenau F, Ultrastructure of Animal Viruses and Bacteriophages: An Atlas. New York: Academic Press. Inc. 1973;5:323-330.
13. Muller G, Bruns M, Martinez Peralta L, Lehmann-Grube F. Lymphocytic choriomeningitis virus. IV. Electron microscopic investigation of the virion. Arch Virol. 1983;75(4):229-42.
14. Murphy FA, Webb PA, Johnson KM, Whitfield SG. Morphological Comparison of Machupo with Lymphocytic Choriomeningitis Virus: Basis for a New Taxonomic Group. J Virol. 1969;4(4):535-41.
15. Murphy FA, Whitfield SG. Morphology and morphogenesis of arena viruses. Bull World Health Organ. 1975;52(4-6):409-19.
16. Walker DH, McCormick JB, Johnson KM, Webb PA, Komba-Kono G, Elliott LH, et al. Pathologic and virologic study of fatal Lassa fever in man. Am J pathol. 1982;107(3):349-56.
17. Morrison H, Goldsmith C, Regnery H, Auperin D. Simultaneous expression of the Lassa virus N and GPC genes from a single recombinant vaccinia virus. Virus Res. 1991;18(2-3):231-41.
18. Tian J, Huang K, Krishnan S, Svabek C, Rowe DC, Brewah Y, et al. RAGE inhibits human respiratory syncytial virus syncytium formation by interfering with F-protein function. J Gen Virol. 2013;94(pt 8):1691-700.
19. Mann E, Edwards J, Brown DT. Polycaryocyte formation mediated by Sindbis virus glycoproteins. J virol. 1983;45(3):1083-9.
20. Murphy SL, Gaulton GN. TR1.3 viral pathogenesis and syncytium formation are linked to Env-Gag cooperation. J Virol. 2007;81(19):10777-85.

21. Landers MC, Dugger N, Quadros M, Hoffman PM, Gaulton GN. Neuropathogenic murine leukemia virus TR1.3 induces selective syncytia formation of brain capillary endothelium. Virol. 2004;321(1):57-64.

22. Hall WC, Kovatch RM, Herman PH, Fox JG. Pathology of measles in rhesus monkeys. Vet Pathol. 1971;8(4):307-19.

23. Chowdhury MI, Koyanagi Y, Suzuki M, Kobayashi S, Yamaguchi K, Yamamoto N. Increased production of human immunodeficiency virus (HIV) in HIV-induced syncytia formation: an efficient infection process. Virus Genes. 1992;6(1):63-78.

24. Wild TF, Malvoisin E, Buckland R. Measles virus: both the haemagglutinin and fusion glycoproteins are required for fusion. J Gen Virol. 1991;72(2):439-42.

25. Higuchi H, Bronk SF, Bateman A, Harrington K, Vile RG, Gores GJ. Viral fusogenic membrane glycoprotein expression causes syncytia formation with bioenergetic cell death: implications for gene therapy. Cancer Res. 2000;60(22):6396-402.

26. Duncan R, Chen Z, Walsh S, Wu S. Avian reovirus-induced syncytium formation is independent of infectious progeny virus production and enhances the rate, but is not essential, for virus-induced cytopathology and virus egress. Virol. 1996;224(2):453-64.

27. Bell TM, Bunton TE, Shaia CI, Raymond JW, Honnold SP, Donnelly GC, et al. Pathogenesis of Bolivian Hemorrhagic Fever in Guinea Pigs. Vet Pathol. 2016;53(1):190-9.

28. Tang DM. Pseudomembranous colitis: not always Clostridium difficile. Cleveland Clinic J Med. 2016;83(5):361-6.

29. Takagi T, Ohsawa M, Yamanaka H, Matsuda N, Sato H, Ohsawa K. Difference of two new LCMV strains in lethality and viral genome load in tissues. Exp Anim. 2017;66(3):199-208.